

Molecular Dynamics Simulations of Thermal Conductivity of Silicon Nanotubes

Yuk Wai Tang¹, Zhen Huang², Xinwei Wang², and X. C. Zeng^{1,*}

¹Department of Chemistry, University of Nebraska-Lincoln, Lincoln, NE 68588-0304

²Department of Mechanical Engineering, University of Nebraska-Lincoln, Lincoln, NE 68588-0656

We use nonequilibrium molecular dynamics simulations to calculate thermal conductivity of single-walled silicon nanotubes (SWSNT). Using a Stillinger and Weber potential for interactions between silicon, we first apply a heat bath—heat sink method on bulk silicon crystal and find that the result of thermal conductivity at a temperature of 500 K that agrees with literature value. We then apply the same method on SWSNT and find that thermal conductivities at temperatures of 400 and 600 K are similar to the bulk case. The results indicate that the phonon transport properties of silicon are not much affected by the nanotube structure.

Keywords: Thermal Conductivity, Molecular Simulations, Silicon Nanotubes.

1. INTRODUCTION

Silicon and related semiconducting materials have been widely used for the manufacturing of computer chips. While advances in technology allow very small chips of high computation power to be made, the efficiency of removing energy from the high density semiconducting materials becomes crucial to prevent overheating of the materials.

To study the energy transport in a material, one can measure the thermal conductivity, κ , of the material by Fourier's law of heat flow, which is given by

$$\kappa = -\frac{J_z}{\partial T / \partial z} \quad (1)$$

where J_z is the heat flux per unit area along the z direction and $\partial T / \partial z$ is the temperature gradient in the same direction.

A number of molecular dynamics simulations have been carried out to study the thermal conductivities of various materials like silicon carbide,¹ silicon crystal,^{2,3} silica,⁴ silicon nanowires,⁵ carbon nanotubes,^{6–8} and model systems such as Lennard-Jones.^{9–12} Two methods are mainly used to determine the thermal conductivity: the Green-Kubo formula¹³ in equilibrium molecular dynamics (EMD) and the non-equilibrium molecular dynamics (NEMD) simulations with heat bath of different temperatures applied onto the system.¹⁴ Each method has its advantages

and weakness. The Green-Kubo method calculates thermal conductivity by means of the energy autocorrelation functions. Since the autocorrelation function is obtained by the energy fluctuation of the molecules, no external and artificial forces are needed. However, a smooth autocorrelation function usually requires an extremely long computing time. Moreover, the long-time region of the autocorrelation function is also difficult to obtain because its small values are interfered by the noise. The function is usually fitted with some exponential function in order to get better results of thermal conductivity. Also, it is not easy to implement the Green-Kubo method in the calculation of thermal conductivity for a system with a quasi-one-dimensional cylinder structure, like a carbon nanotube. This is because there is a lot of empty space around the tube and the vibration frequency of atoms in radial and axial direction of the tube is not the same. Since the cylinder structure is not homogeneous in all three dimensions, it is not straightforward to apply the Green-Kubo method without major modification.

The NEMD method is an experiment-like method. An energy flux is generated by either imposing the heat flux on selected slabs or by temperature rescaling. The method is feasible only when a linear temperature gradient is generated. A large temperature gradient is usually needed in order to observe the gradient over the fluctuation of temperature. This gradient is astronomical when applied on a nanoscale system. Both EMD and NEMD methods can be affected by the material size. However, NEMD method normally requires a much larger system size than the EMD method.³ The values of thermal conductivity are reduced

when the mean free path is comparable to the size of the system. Recent proposed simulations of band gap materials sized in nanoscale conductive fundamental the studies as well as the silicon in simulation deploy the activity of the configurational

2. SIMULATION

Classical molecular dynamics simulation interaction potential,¹

$$U_2(r)$$

where A , B , C , D , E , F , G , H , I , J , K , L , M , N , O , P , Q , R , S , T , U , V , W , X , Y , Z are the parameters between given by,

$$U_3(r)$$

where θ_{ijk} is the angle between the vectors \mathbf{r}_{ij} and \mathbf{r}_{ik} , etc. The value of θ_{ijk} is given by,

$$h(r_{ij}, r_{ik})$$

where λ are the parameters used in Eq. (2).

Table I.

Symbol
A
B
p
q
a
λ
γ

*Author to whom correspondence should be addressed.

when the size of simulated systems is comparable to the mean free path of phonons.

Recently, single-walled silicon nanotubes have been proposed by computer simulations.^{15–17} *Ab initio* calculations of the silicon nanotubes show that they have zero band gap and thus are metals rather than semiconducting materials. Although the nanotubes have not been synthesized in laboratories, theoretical studies of their thermal conducting properties can lead to better understanding of fundamental behavior of the silicon nanostructures. Also, the studies can provide more information for the synthesis as well as for potential application in future.

In this paper, we compare thermal conductivity of bulk silicon in various temperatures and sizes using NEMD simulations with previous literature results. Then, we deploy the same technique to study the thermal conductivity of single-walled silicon nanotubes using equilibrium configurations.

2. SIMULATION TECHNIQUES

Classical MD simulations were used in the study of thermal conductivities of silicon materials. The silicon–silicon interactions are described by the Stillinger and Weber potential,¹⁸ with pair potential,

$$U_2(r) = \begin{cases} A(Br^{-p} - r^{-q}) \exp[(r-a)^{-1}], & r < a \\ 0, & r \geq a \end{cases} \quad (2)$$

where A , B , p , a are positive parameters and r is the distance between two atoms. The three-body interactions are given by,

$$U_3(\mathbf{r}_i, \mathbf{r}_j, \mathbf{r}_k) = h(r_{ij}, r_{ik}, \theta_{jik}) + h(r_{ji}, r_{jk}, \theta_{ijk}) + h(r_{ki}, r_{kj}, \theta_{ikj}) \quad (3)$$

where θ_{jik} is the angle between \mathbf{r}_j and \mathbf{r}_k subtended at vertex i , etc. The function h belongs to a two-parameter family. When both r_{ij} and r_{ik} are less than a , h has the form,

$$h(r_{ij}, r_{ik}, \theta_{jik}) = \lambda \exp[\gamma(r_{ij} - a)^{-1} + \gamma(r_{ik} - a)^{-1}] \times (\cos \theta_{jik} + 1/3)^2 \quad (4)$$

where λ and γ are constant. The value of the parameters used in Eqs. (2) to (4) are listed in Table I. Both the

Table I. Parameters in the Stillinger and Weber potential.

Symbol	Reduced unit	Real unit
A	7.049556277	1474.8 kJ mol ⁻¹
B	0.6022245584	—
p	4	—
q	0	—
a	1.80	0.37712 nm
λ	21.0	4393.2 kJ mol ⁻¹
γ	1.20	—

reduced unit and the real unit (if any) of the parameters are listed and the absolute values for size and energy are:

$$\sigma = 2.0951 \text{ \AA}$$

$$\varepsilon = 209.2 \text{ kJ mol}^{-1}$$

2.1. Calculating Thermal Conductivities

We use NEMD simulations to calculate thermal conductivity in the way of imposing heat slabs of different temperatures to the system. One of the common ways to calculate thermal conductivity is by Jund's method.⁴ However, such a method has been used on structures with periodic boundary conditions only. As we are dealing with systems with periodic boundary conditions as well as finite-size nanostructures, we employed an alternate method originally developed by Rapaport¹⁹ with a modification in the way the molecules are rescaled. There are two ways of doing the simulation with the Rapaport's method, depending on the system. For a *finite* system, we apply heat bath on the walls at both ends of one dimension of the simulation box. In the Rapaport's method, when a particle reaches the wall, it is reflected and its velocity is rescaled to the temperature of the heat wall.¹⁹ This method generates a two-dimensional environment in the simulation box (Fig. 1a). The thermal conductivity Eq. (1) is rewritten as,

$$\lambda = \frac{\Delta E_{\text{heat}} + \Delta E_{\text{cold}}}{2tA \partial T / \partial z} \quad (5)$$

where ΔE_{heat} and ΔE_{cold} are the changes of kinetic energy of atoms after their velocities are rescaled, t is the time step interval and A is area of cross section. In our simulation of a nanotube, the velocities of atoms located within a fixed distance from one end are rescaled while they are not subject to the imaginary wall on both ends. In this way, the nanotube length will be more flexible and its length can be changed.

For a system with three-dimensional periodic boundary conditions, the heat slabs of a certain thickness are located at a distance of $L/4$ from each side of the simulation box (Fig. 1b).²⁰ When molecules enter the slabs, their velocities are rescaled according to the temperature of the slabs. In this case, periodic boundary conditions are applied on all three dimensions and symmetry of the system is retained. The equation of thermal conductivity in this case is written as,

$$\lambda = \frac{\Delta E_{\text{heat}} + \Delta E_{\text{cold}}}{4tA \partial T / \partial z} \quad (6)$$

where ΔE_{heat} and ΔE_{cold} are the changes of kinetic energy of atoms after their velocities are rescaled with the heat slabs. Note that the right hand of equation is divided by a factor of 4 instead of 2 in Eq. (5) because the heat flux goes to two directions (one via the periodic boundary) from the hot plate to the cold plate.

In the simulations, the heat exchange between molecules and the heat slabs are done by assigning new velocities to the molecules involved. Using Boltzmann distribution

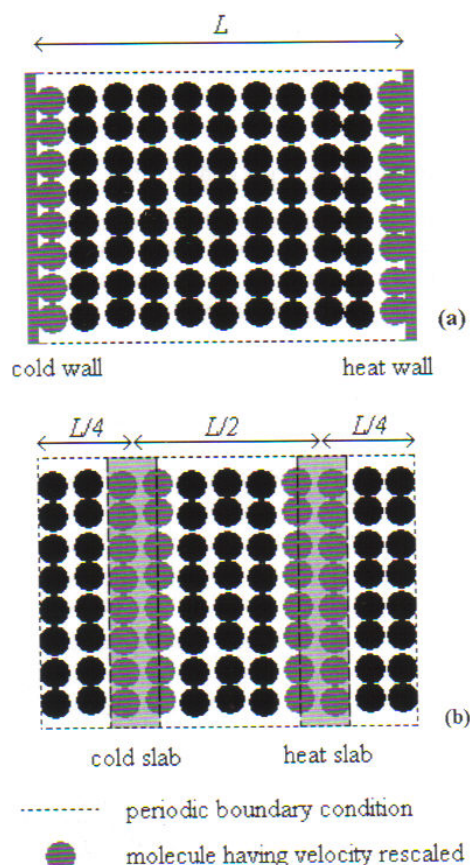


Fig. 1. Illustration of heat-bath and heat-sink method to calculate thermal conductivity for: (a) Low-dimension system in nanotube and (b) 3D system in bulk silicon phase. Note in case (a), the 'wall' is not fixed in dimension.

function of kinetic energy,

$$\frac{1}{2} \sum_{i=1}^N m_i v_i^2 = \frac{3}{2} N k_B T \quad (7)$$

where m_i and v_i are the mass and velocity of particle i , N the number of molecules in the system, k_B the Boltzmann constant, and T the temperature. The assigned constant velocity, v , of molecules is,

$$v = \sqrt{\frac{3k_B T_p}{m}} \quad (8)$$

where T_p is the temperature of the heat plate. The change of heat flux can be found by calculating the difference of kinetic energy before and after velocity rescaling. Moreland and co-workers suggested using Berendsen and Andersen thermostats for velocity rescaling so that a weak relaxation time can be chosen and interference of the phonon behavior by the abrupt rescaling of velocities can be minimized.⁸ We did not use Berendsen or Andersen thermostat in our simulation. Instead, we rescale the velocities of molecules every certain time interval.

We carried out simulations on bulk silicon crystal at a temperature of 500 K and applied the temperature rescaling in different time intervals from 0.5 fs to 400 fs. We found that the thermal conductivity results are independent of the rescaling time intervals if they are between 25 and 400 fs. In the simulations, we applied the velocity rescaling every 100 fs for all models and conditions.

3. RESULTS AND DISCUSSION

3.1. Bulk Crystalline Silicon

The simulation of bulk silicon requires setup of a diamond-structure crystal lattice. We constructed several structures with a uniform cross sectional dimension of 4×4 cell units. The z -dimension, in which the length between the heat source and heat sink is measured, varies from 12 to 200 units. The values of the setup are shown in Table II. A special cell with a dimension of $20 \times 20 \times 20$ and contains 64,000 atoms is constructed to compare with the EMD result done by Voltz et al.² Periodic boundary conditions were applied on all three dimensions and the lattice constant is 5.43 Å. The simulations were run at a temperature of 500 K. Nose-Hoover thermostat is used with a fifth-order Gear's predictor and corrector algorithm to maintain the system at constant temperature at the beginning. The NVT simulation lasts for at least 0.1 ns to assure equilibration. Then the system was run in NVE ensemble for an additional short run (0.1 ns) before the temperature rescaling and measurement of temperature gradient took place. The heat slab method (Fig. 1b) was used to find the thermal conductivity.

Figure 2 shows a temperature profile of bulk silicon simulated at a temperature of 500 K. The temperature gradient was measured from the linear response region of the temperature profile. Thermal conductivity was calculated using Eq. (6). For the $4 \times 4 \times 96$ system, the value of thermal conductivity, after running 2 ns, is 66.7 ± 10 W/mK, while for the smallest ($4 \times 4 \times 12$) and largest system ($4 \times 4 \times 200$) considered, 5 ns and 1 ns were used to compute the thermal conductivity. The percentage error is about the same as previous literature of NEMD results.³

Figure 3 shows the result of thermal conductivity for different cell dimensions. The value of thermal conductivity of bulk silicon at 500 K becomes leveled when the length of simulation cell is 50 nm or more. Our NEMD results of bulk silicon are consistent with previous ones obtained from a large-scale EMD simulation.² These results are also in reasonable agreement with the experimental value.²⁰

Table II. Setup of bulk silicon crystals.

Cell unit	z dimension length (nm)	No. of atoms
$4 \times 4 \times 12$	6.516	1,536
$4 \times 4 \times 96$	52.13	12,288
$4 \times 4 \times 200$	108.6	25,600
$20 \times 20 \times 20$	10.86	64,000

Temperature (K)

Fig. 2.

However, another system, of different size, which at the same time step we apply to obtain time flux. As it entails calculated function the Jund calculate present the pressure (see the

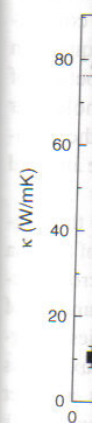


Fig. 3. The source of re

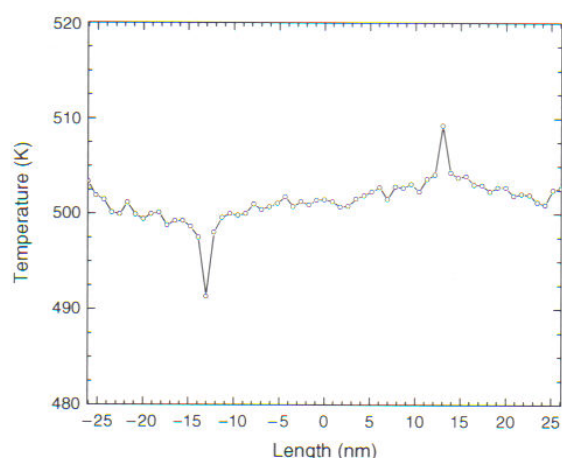


Fig. 2. Temperature profile along the cross section of silicon crystal.

However, our results are appreciably larger compared with another NEMD results³ with the same given length of the system. This large discrepancy is likely due to the use of different methodology in calculating thermal conductivity. The previous NEMD study³ adopted Jund's method⁴ which applies a fix amount of heat to the system in every time step and then calculates temperature gradient, while we applied the heat by rescaling the temperature at certain time intervals and then calculated the change of heat flux. As pointed out by Schelling et al.³ that Jund's method entails severe finite-size effects. In other words, the calculated thermal conductivity converges very slowly as a function of system size. The severe finite-size effects with the Jund's method may explain the large discrepancy in the calculated thermal conductivity when compared with the present one as the same given system size. Note also that the present NEMD method can be extended straightforwardly to finite-size systems, e.g., a finite-length nanotube (see the section below).

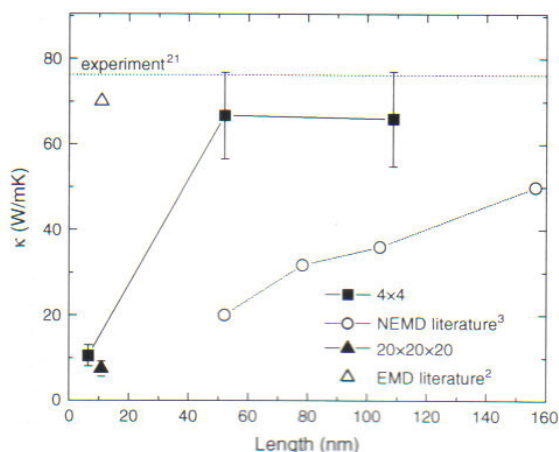


Fig. 3. Thermal conductivity of bulk silicon at 500 K. Refer to the source of references for the numbers in superscript.

Finally, we find that thermal conductivity for the system with a dimension of $20 \times 20 \times 20$ is about 10% the value calculated by EMD simulation.² We thus conclude that while calculation of thermal conductivity by Green-Kubo's method depends on the size in all dimensions, the calculation by the present NEMD method depends on the *length of the side* where temperature gradient is measured.

3.2. Silicon Nanotubes

The simulations of silicon nanotubes were technically more difficult to do because the long nanotube structure of silicon is less stable than other phases and the actual model has not yet been discovered in real experiment. We performed calculation on the pentagon cross section model, which is found to be the most stable structure among the single-walled silicon nanotubes in a previous study.²⁰

The initial configuration of silicon nanotube was generated by repeating the unit cell structure in the axial direction. The length of the nanotube varies from 47.5 nm to 477 nm. For a silicon nanotube with a length of 47.5 nm, it consists of 200 layers of silicon atoms arranged in a pentagon cross-section.

The silicon nanotube was brought to equilibrium by running MD simulations in NVT ensemble for 1 ns. Nose-Hoover thermostat was used to maintain a constant temperature. After that, the system was run in NVE for further 1 ns. Then a heat bath was introduced in one end of the tube and a heat sink the other end. Temperature gradient along the tube and change of heat flux were measured. Thermal conductivity along the axial direction of the tube was calculated using Eq. (5). Finite sizes of tubes are used and no periodic boundary conditions were applied. It allows the tubes to relax and dissipate heat resulted from torsional motion.

The cross-sectional area is a pentagon ring and its definition is illustrated in Figure 4. The definition is similar to how the cross-section area is defined in a single-walled carbon nanotube.⁸ The thickness of the pentagon ring is equal to the bond length between two silicon atoms and is

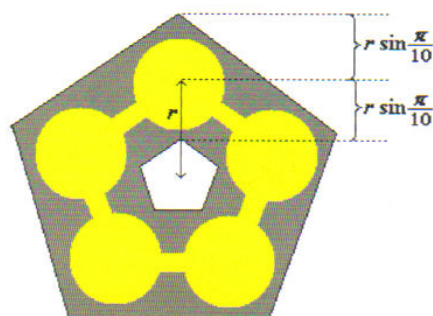


Fig. 4. Definition of cross-section area of a silicon nanotube. The value of $r \sin(\pi/10)$ is equivalent to half the length of Si-Si bond forming the pentagon. The shaded area is the cross section area in calculating thermal flux.

Table III. Simulation details and results of thermal conductivity of silicon nanotubes at 400 and 600 K. Data shown in the table are: Temperature, T ; Cross-sectional area, A ; Length of nanotubes, l ; Number of atoms, N ; Simulation time, t ; and thermal conductivity, κ .

T (K)	A (nm ²)	l (nm)	N	t (ns)	κ (W/mK)
400	0.2398	47.5	1000	10	28.7 ± 6.0
		190.6	4000	10	26.4 ± 8.6
		476.7	10000	10	66.5 ± 23
600	0.2412	47.5	1000	10	25.1 ± 7.2
		95.2	2000	15	24.4 ± 5.1
		190.6	4000	10	25.1 ± 8.2
		476.7	10000	10	40.9 ± 33

approximately the van der Waals thickness of silicon. The tube radius, r , defined in the figure depends on the bond length between two silicon atoms located on the same pentagonal plane and it increases slightly with increasing temperature.

Thermal conductivity of silicon nanotube at temperatures of 400 and 600 K were shown in Table III. The results were obtained from at least 10 ns of simulation. Thermal conductivity increases with the length of the tube. Conductivity decreases with temperature, which has the same behavior as in the bulk phase, and the values are similar to the bulk phase result. The result suggests that the phonon behavior of silicon atoms in a nanotube structure is similar to those in a bulk phase. The thermal conductivity data for the long tubes have a larger error. We anticipate that much longer simulation time than 10 ns is required for a long silicon nanotube due to the greater chance for a twisting phenomenon as a result of torsional force, which may contribute to the error in the measurement of temperature along the tube.

Temperature profile along a silicon nanotube was shown in Figure 5. Temperature increases generally along the nanotube when the heat bath is applied. Figure 6 shows thermal conductivity of silicon nanotube of different lengths and at temperatures of 400 and 600 K. The result

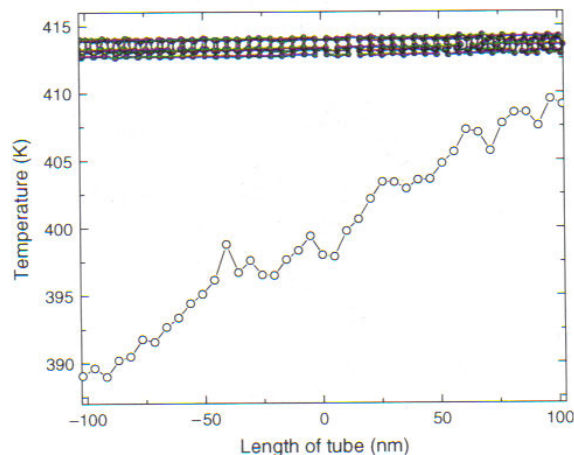


Fig. 5. Temperature profile along a silicon nanotube at equilibrium temperature of 400 K.

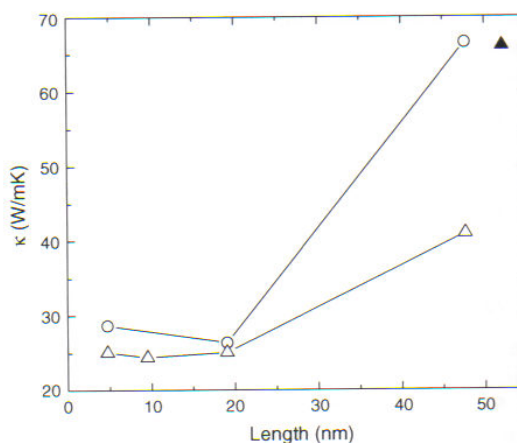


Fig. 6. Tube length dependent of thermal conductivity of single-walled silicon nanotube at temperatures of: 400 K (circle) and 600 K (triangle). The value for bulk silicon at 500 K (solid triangle) is also shown.

of bulk silicon at a temperature of 500 K is also shown in a solid triangle symbol. The values of thermal conductivity of silicon nanotube by molecular simulation are found to be similar to those in corresponding bulk phase. This suggests that silicon atoms in the silicon nanotube have similar phonon type heat transfer ability as when they are arranged in crystalline structure. It looks as if the tube structure does not have special effect on the thermal transport. However, if the comparison is based on the same density assumption by bundling several silicon nanotubes so that they have a same density as in bulk silicon, their thermal conductivity could be very different. A preliminary simulation shows that silicon nanotube bundle shows a lower thermal conductivity than bulk silicon.

Since only classical simulations were carried out in this study, it is not surprising that the results of thermal conductivity cannot reveal the metallic properties of silicon nanotube and the contribution of thermal transport by other media such as electrons. In order to calculate the amount of contribution by electrons to thermal conductivity, we need to perform a quantum or quasi-quantum mechanics calculation which considers the distribution of electrons. A tight-binding²² or Car Parrinello²³ molecular dynamics simulation may do the trick, although the accuracy of results are not ensured when a long time interval simulation is performed.

The cross sectional area may also contribute to the similarity between values of thermal conductivity of silicon nanotube and silicon crystals. The definition of cross sectional area is an estimate of the Lennard-Jones boundary of the atoms. Each atom in a silicon nanotube carries a bigger cross sectional area and this makes energy flux across the tube lower. Also, a pentagon structure has a lower molecule density and a larger surface area than a bulk crystalline structure. This may result in a heat loss during the measurement of heat flux and a decrease in the value of thermal conductivity.

4. CONCLUSION

We carried out NEMD simulations to calculate thermal conductivity for both bulk silicon crystals and single-walled silicon nanotubes using the Fourier's law. Thermal conductivity of bulk silicon at a temperature of 500 K is in reasonable agreement with experimental values. Thermal conductivity of silicon nanotubes at temperatures between 400 K and 600 K show little discrepancies from the bulk phase at similar temperature. It suggests that the phonon vibrations in silicon are not much affected by atomic structure. Other forms of thermal conduction, such as conduction by electron, cannot be shown by classical simulation and we must resort to computer simulations with quantum mechanical factors.

Acknowledgments: We thank Dr. Vijay Kumar and Dr. Jaeil Bai for valuable discussions. This research was supported by grants from DOE (DE-FG02-04ER46164), NSF (CHE, DMII, and MRSEC), the John Simon Guggenheim Foundation, and Nebraska Research Initiatives (X. C. Z.) and by the Research Computing Facility and Research Council of University of Nebraska-Lincoln.

References

1. J. Li, L. Porter, and S. Yip, *J. Nuclear Mater.* 255, 139 (1998).
2. S. G. Volz and G. Chen, *Phys. Rev. B* 61, 2651 (2000).
3. P. K. Schelling, S. R. Phillpot, and P. Keblinski, *Phys. Rev. B* 65, 144306 (2002).
4. P. Jund and R. Jullien, *Phys. Rev. B* 59, 13707 (1999).
5. S. G. Volz and G. Chen, *Appl. Phys. Lett.* 75, 2056 (1999).
6. S. Berber, Y. K. Kwon, and D. Tománek, *Phys. Rev. Lett.* 84, 4613 (2000).
7. S. Maruyama, *Microscale Therm. Eng.* 7, 41 (2003).
8. J. F. Moreland, J. B. Freund, and G. Chen, *Microscale Therm. Eng.* 8, 61 (2004).
9. R. Vogelsang, C. Hoheisel, and G. Ciccotti, *J. Chem. Phys.* 86, 6371 (1987).
10. F. Muller-Plathe, *J. Chem. Phys.* 106, 6082 (1997).
11. H. Kaburaki, J. Li, and S. Yip, *Mater. Res. Soc. Symp. Proc.* 538, 503 (1998).
12. A. J. H. McGaughey and M. Kaviani, *Int. J. Heat and Mass Transfer* 47, 1783 (2004).
13. R. H. Poetzsch and H. Böttger, *Phys. Rev. B* 50, 15757 (1994).
14. A. Tenenbaum, G. Ciccotti, and R. Gallico, *Phys. Rev. A* 25, 2778 (1982).
15. J. Bai, X. C. Zeng, H. Tanaka, and J. Y. Zeng, *Proc. Natl. Acad. Sci. USA* 101, 2664 (2004).
16. A. K. Singh, V. Kumar, T. M. Briere, and Y. Kawazoe, *Nano Lett.* 2, 1243 (2002).
17. A. N. Andriotis, G. Mpourmpakis, G. E. Froudakis, and M. Menon, *New J. Phys.* 4, 78 (2002).
18. F. H. Stillinger and T. A. Weber, *Phys. Rev. B* 31, 5262 (1985).
19. D. C. Rapaport, *The Art of Molecular Dynamics Simulation*, 2nd edn., Cambridge University Press, Cambridge (2004).
20. H. Kaburati and M. Machida, *Phys. Lett. A* 181, 85 (1993).
21. D. R. Lide, *CRC Handbook of Chemistry and Physics*, 82nd edn., CRC Press, Boca Raton (2001).
22. C. Z. Wang, C. T. Chan, and K. M. Ho, *Phys. Rev. B* 42, 11276 (1990).
23. R. Car and M. Parrinello, *Phys. Rev. Lett.* 55, 2471 (1985).

Received: 17 May 2005. Accepted: 18 July 2005.